Microscopic model for the frustrated Cu II-spin tetrahedron-based $Cu_4Te_5O_{12}X_4$ (X=Cl, Br) systems

Badiur Rahaman,[1] Harald O. Jeschke,[2] Roser Valentí,[2] and T. Saha-Dasgupta[1]
[1]*S.N. Bose National Centre for Basic Sciences, JD Block, Sector 3, Salt Lake City, Kolkata 700098, India*
[2]*Institut für Theoretische Physik, Universität Frankfurt, Max-von-Laue-Strasse 1, 60438 Frankfurt, Germany*
(Received 21 August 2006; published 5 January 2007)

We present a microscopic study of the electronic and magnetic properties of the recently synthesized spin tetrahedron system $Cu_4Te_5O_{12}Cl_4$ based on density functional calculations and on *ab initio*-derived effective models. In view of these results, we discuss the origin of the observed differences in behavior between this system and the structurally similar $Cu_2Te_2O_5Cl_2$. Since the Br analog of the title compound has not been synthesized yet, we derive the crystal structure of $Cu_4Te_5O_{12}Br_4$ by geometry optimization in an *ab initio* molecular dynamics calculation and investigate the effect of substituting Cl by Br. The possible magnetic behavior of $Cu_4Te_5O_{12}Br_4$ in comparison with the recently studied $Cu_2Te_2O_5Br_2$ is also discussed.

DOI: 10.1103/PhysRevB.75.024404 PACS number(s): 75.10.Jm, 71.15.Mb

INTRODUCTION

Frustrated magnetism has gained a lot of attention in recent years due to the wealth of exotic behavior that arises out of this condition such as spin ice and spin liquid phases.[1] In the search for new materials exhibiting frustrated magnetism, a few years ago Johnsson *et al.*[2] synthesized a family of oxohalogenides $Cu_2Te_2O_5X_2$, X=Br, Cl whose structure was based on weakly coupled tetrahedra of CuII with geometrically frustrated antiferromagnetic interactions. These materials have been intensively studied both experimentally and theoretically.[3–6,8–11] They show magnetic ordering with incommensurate wave vectors at temperatures T_N=18 K (Cl) and 11 K (Br) and the observation of a longitudinal magnon[5] in $Cu_2Te_2O_5Br_2$ was interpreted as evidence for the proximity of this system to a quantum phase transition between antiferromagnet and spin liquid behavior.

The various intratetrahedral and intertetrahedral couplings and the relative strengths of exchange pathways in these compounds have been obtained in detail[6] by using the electronic structure technique of muffin-tin orbital (MTO) based *N*MTO-downfolding.[12] The results predicted by this study have been confirmed by subsequent neutron diffraction experiments[13] proving the powerfulness of this *ab initio* density functional theory based method in predicting the underlying microscopic model of a complex material.[7]

By changing the subtle ratio between the various interaction paths in these materials, for instance by applying pressure or by introducing chemical modifications,[14–16] one can attempt to drive these systems into quantum criticality. Following these ideas, an oxohalogenide $Cu_4Te_5O_{12}Cl_4$ has been very recently synthesized by Takagi *et al.*[17] which orders antiferromagnetically at T_N=13.6 K. This system is structurally similar to the previously discussed $Cu_2Te_2O_5Cl_2$ but presents some markedly different features. As pointed out by Takagi *et al.*, the primary structural difference between the $Cu_4Te_5O_{12}Cl_4$ [which we refer to as Cu-45124(Cl) following Ref. 17] and $Cu_2Te_2O_5Cl_2$ [Cu-2252(Cl)] is the presence of a TeO_4 complex in the middle of the Cu-tetrahedral network in the *ab* plane (see Fig. 1). This fact led the authors of Ref. 17 to expect an increase in the separation between the Cu_4 tetrahedra and hence an increase in the relative importance of the intratetrahedral coupling with respect to the intertetrahedral coupling.

In the following, we study this proposition within the framework of the *N*MTO-downfolding technique. In addition, motivated by the more anomalous properties of $Cu_2Te_2O_5Br_2$ compared to $Cu_2Te_2O_5Cl_2$ as reported in the literature,[3–6,8–11,14,15] we explore the implications of substituting Cl with Br in Cu-45124(Cl). Since the Cu-45124(Br) system has not been synthesized yet, we propose the crystal structure of $Cu_4Te_5O_{12}Br_4$ by performing a geometry relaxation in the framework of *ab initio* molecular dynamics and we analyze its electronic structure by the *N*MTO-downfolding technique.

STRUCTURE

Both Cu-45124(Cl) and Cu-2252(Cl) compounds crystallize in a tetragonal structure. The basic structural unit in both systems is the $[CuO_3Cl]$ distorted square (marked by thin lines in Fig. 1) with Cu (marked in magenta in Fig. 1) at the center. Groups of four such squares share corners, giving rise to $[Cu_4O_8Cl_4]$ units with Cu ions in tetrahedral coordination. Cu-45124(Cl) has two inequivalent Te atoms, Te(1) and Te(2) (marked in black and yellow in Fig. 1 top panel), while Cu-2252(Cl) has only one type of Te atom (marked in yellow in Fig. 1 bottom panel). The Te(2) atoms in Cu-45124(Cl) sit on an equivalent position to the Te atoms in Cu-2252(Cl). Viewing the structures along the [001] direction (see Fig. 2), they show a stacking of Cu_4 tetrahedra separated by layers of Te(2)-O(3) [Cu-45124(Cl)] or Te-O(2) [Cu-2252(Cl)] units. In the case of Cu-45124(Cl), additional Te(1)-O(1) units appear in the same layer as Cu. The relative orientation of the Cu_4 tetrahedra along the [001] direction is also different between the two compounds. In the case of Cu-2252(Cl) the Cu_4 tetrahedra show the same orientation, while for Cu-45124(Cl) they alternate between successive rows. The latter feature leads to two different space group symmetries, $P\bar{4}$ for Cu-2252(Cl) and $P4/n$ for Cu-45124(Cl) with elongation of the unit cell in the *ab* plane with lattice parameter *a*

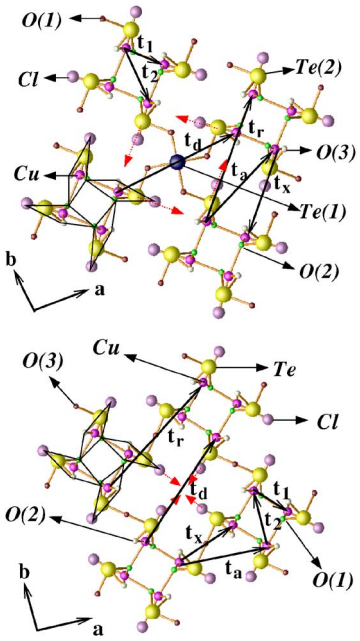

FIG. 1. (Color online) Crystal structure of Cu-45124(Cl) (top panel) and Cu-2252(Cl) (bottom panel) projected on the *ab* plane. In order to emphasize the similarity between the Cu-2252(Cl) and Cu-45124(Cl) structures, we use four unit cells of Cu-45124(Cl) but show only the section that makes this structure analogous to a section of four Cu-2252(Cl) unit cells showing four connected Cu tetrahedra. The balls representating various atoms are of varying sizes, Te being the largest, and Cl, Cu, and O in order of decreasing sizes. Magenta (dark gray) and pink (gray) atoms stand for Cu and Cl. Two inequivalent Te atoms, Te(1) and Te(2) in Cu-45124(Cl) are shown in deep blue (black) and yellow (light gray) colors (top panel), while the only one inequivalent Te atom present in Cu-2252(Cl) is shown in yellow (light gray) color (bottom panel). The smallest brown (black), green (gray) and white (white) balls denote O(1), O(2), and O(3), respectively, for Cu-45124(Cl) (top panel) and O(3), O(1), and O(2) for Cu-2252(Cl) (Ref. 18). Note that every four Cu atoms appearing in a square arrangement, due to the projection, actually form tetrahedra. We also show the various interaction paths in black arrows (see the text for discussion).

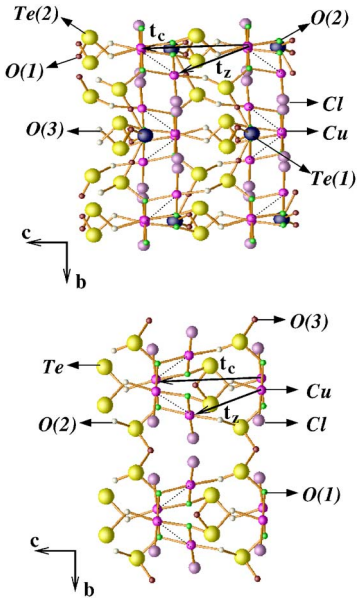

FIG. 2. (Color online) View of the crystal structure of the Cu-45124(Cl) (top panel) and Cu-2252(Cl) (bottom panel) compounds along the [001] direction. Color scheme and the convention for ball sizes is the same as in Fig. 1. The thick arrows denote the various interaction paths.

$=11.35$ Å for Cu-45124(Cl) compared to $a=7.84$ Å for Cu-2252(Cl). The unit cell dimensions along the c axis remain comparable with $c=6.32$ Å for Cu-2252(Cl) and $c=6.33$ Å for Cu-45124(Cl). The change in space group defines Cu-45124(Cl) as centrosymmetric compared to the noncentrosymmetric Cu-2252(Cl).

A crucial difference between the two compounds, apart from the change in bond lengths, is the relative orientation of the Cu-Cl bonds (Cl atoms are marked in pink in Fig. 1) among different Cu_4 tetrahedra. As has been discussed in Ref. 6, the Cl atoms play an important role in mediating the Cu-Cu interaction in the Cu-2252 systems. While for Cu-2252(Cl) the Cu-Cl bonds belonging to different Cu_4 tetrahedra point toward each other (marked with red arrows in Fig. 1 bottom panel), in the case of Cu-45124(Cl), due to the relative shift of the tetrahedra, they are oriented parallel to each other (see the red arrows in Fig. 1 top panel). This aspect is found to have important consequences in the context of hopping interaction pathways, as will be discussed later.

BANDSTRUCTURE

Figure 3 shows the non-spin-polarized band dispersion of Cu-45124(Cl) obtained with the linear muffin-tin orbital basis[19] within the framework of local density approximation (LDA). The bands are plotted along the various symmetry directions of the tetragonal Brillouin zone. The orbital characters indicated in the figure are obtained by choosing the local coordinate system with the y axis pointing along the Cu-O(3) bond and the x axis pointing along the Cu-Cl bond. The square planar symmetry of the ligands surrounding the Cu^{2+} ion sets the Cu-$3d_{x^2-y^2}$ energy level as the highest energy level. Consistent with the Cu^{2+} valency, eight bands (there are eight Cu atoms in the unit cell) dominated by Cu-$d_{x^2-y^2}$ character and split off from the rest of the bands, span an energy range from ≈ -0.3 to 0.2 eV with the zero of energy set at the LDA Fermi level. The energy bands dominated by other d characters like d_{xy}, d_{zx}, d_{yz}, and d_{3z^2-1} are located in the energy range between ≈ -3 and -2 eV overlapping with the O-p manifold. The Cl-p dominated bands appear right above and partly overlapping the O-p bands within an energy range of ≈ 1 eV. These Cl-p dominated bands are separated by a gap of ≈ 0.5 eV from the Cu-$d_{x^2-y^2}$ dominated bands. There is only a negligible contribution of Te(1) and Te(2) to the bands crossing the Fermi energy. We note that in the low-energy scale, the LDA calculation leads to eight almost half-filled bands, i.e., to a metallic state. Introduction of correlation effects within an LDA+U treatment are expected to drive the system insulating. In what follows though we will focus on the *ab initio* determi-

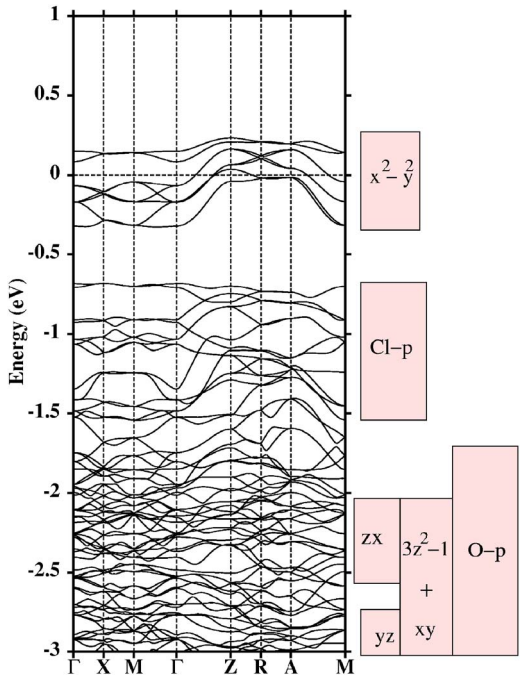

FIG. 3. (Color online) LDA band dispersion of Cu-45124(Cl) plotted along various symmetry directions with $\Gamma=(0,0,0)$, $X=(\pi,0,0)$, $M=(\pi,\pi,0)$, $Z=(0,0,\pi)$, $R=(0,\pi,\pi)$, and $A=(\pi,\pi,\pi)$. The dominant orbital contributions in various energy ranges are shown in small boxes drawn on the right-hand side.

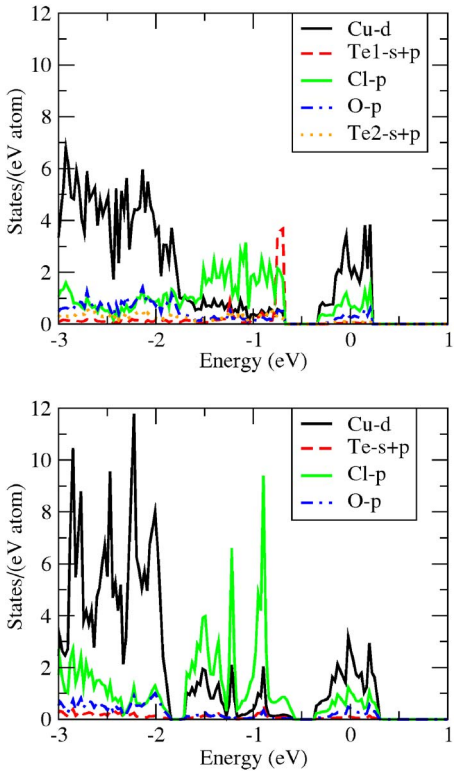

FIG. 4. (Color online) Comparison of the density of states between the Cu-45124(Cl) (top panel) and Cu-2252(Cl) (bottom panel) compounds.

nation of effective one-electron hopping interactions which are well described within LDA and generalized gradient approximation (GGA).

In Fig. 4 we show a comparative study of the various partial LDA density of states (DOS) for Cu-45124(Cl) and Cu-2252(Cl).

While the basic features of the DOS remain the same between the two compounds—indicating that the overall nature of the interactions will be similar for both systems—there are a few quantitative differences. The Cu-d bandwidth at E_F is narrower in Cu-45124(Cl) than in Cu-2252(Cl). The relative proportion of the Cl-p and O-p contribution to the bands at E_F is also smaller in the case of Cu-45124(Cl). The O-p and Cl-p dominated bands, instead of being separated, overlap to a larger extent in the case of Cu-45124(Cl). Understanding and quantifying these differences requires the analysis of the bandstructure in terms of a microscopic model.

DOWNFOLDING AND EFFECTIVE MODEL

A powerful technique to construct a low-energy, tight-binding (TB) Hamiltonian starting from a complex LDA bandstructure is achieved via the *N*MTO-downfolding technique. It does so by constructing energy-dependent, effective orbitals by integrating out irrelevant degrees of freedom—a method called *downfolding*. The accuracy of such a procedure can be tuned by the choice of N, the number of energy points used in the *N*MTO calculation. For an isolated set of bands, as is the case in the present study, these effective orbitals define the Wannier functions corresponding to the Hamiltonian in the downfolded representation. The real space representation of the downfolded Hamiltonian in the Wannier function basis gives the information of the effective hopping matrix elements.

For the present study, we construct the massively downfolded Hamiltonian by keeping only the Cu-$d_{x^2-y^2}$ degrees of freedom active and integrating out all the rest. The computed, downfolded bands are shown in the top panel of Fig. 5 with solid lines. With the choice of two energy points, E_0 and E_1, the downfolded bands are indistinguishable from the Cu-$d_{x^2-y^2}$ dominated bands of the full LDA calculation shown in dashed lines in the top panel of Fig. 5.

The corresponding Wannier function is plotted in Fig. 6. Two different views of the same orbital are shown. The central part has the $3d_{x^2-y^2}$ symmetry with the choice of the local coordinate system as stated above, while the tails are shaped according to Cl-p_x and O-p_x/p_y symmetry demonstrating the hybridization effects. The strong $pd\sigma$ antibonds are evident in the plot with Cu hybridization being stronger with Cl than with O, a fact also evident in the density of states plot, shown in Fig. 4.

The real space representation of the downfolded Hamiltonian in the Wannier function basis, $H_{TB}=-\Sigma_{ij}t_{ij}(\hat{c}_i^\dagger\hat{c}_j+\text{h.c.})$ provides the information of the effective hopping interaction t_{ij}, between the Cu^{2+} ions at sites i and j. The various dominant hopping interactions are tabulated in Table I. The notation for the hoppings are shown in Figs. 1 and 2. While the hoppings t_1, t_2, t_x, t_a, and t_r are in-plane hoppings

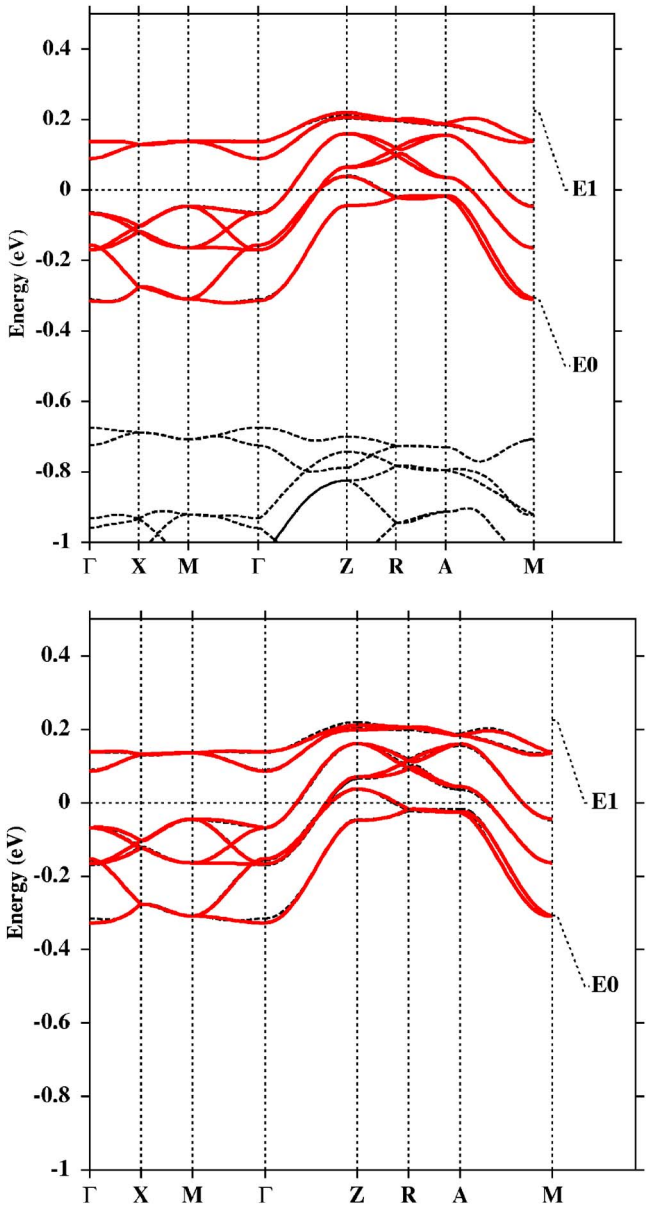

FIG. 5. (Color online) Top panel: Bands obtained with massively downfolded Cu-$d_{x^2-y^2}$ basis (in solid lines) compared to full LDA band structure (in dashed lines). The *N*MTO energy points E_n spanning the region of interest are shown on the right-hand side. Bottom panel: The tight-binding bands obtained with the hopping interactions shown in Table I (in dashed lines) compared with downfolded bands (in solid lines).

in the plane defined by the Cu tetrahedra, t_z and t_c are out-of-plane hoppings. For the sake of consistency, we adopt for Cu-45124(Cl) the same hopping notation introduced earlier for Cu-2252(Cl) in Ref. 6.

For comparison, in Table I we reproduce the results for the Cu-2252(Cl) compound from Ref. 6. The bond lengths corresponding to each hopping element have been also tabulated. For the dominant, intratetrahedral nearest-neighbor interaction, t_1, we observe that while the bond length is decreased by only 2.5% for Cu-45124(Cl) compared to Cu-2252(Cl), t_1 is reduced by as much as 22% due to a smaller superexchange path angle in Cu-45124(Cl) [$\angle$Cu-O(2)-Cu

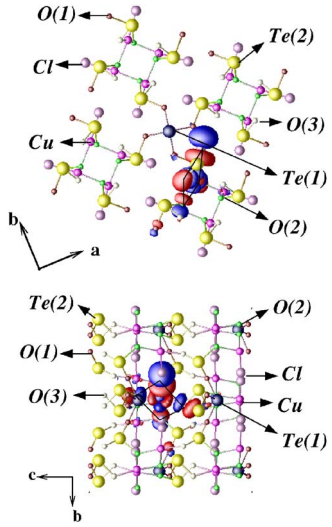

FIG. 6. (Color online) Effective orbital corresponding to massively downfolded Cu-$d_{x^2-y^2}$ calculation viewed in two different planes. Plotted are the orbital shapes (constant-amplitude surfaces) with lobes of opposite signs colored as red (gray) and deep blue (black). The $d_{x^2-y^2}$ orbital is defined with the choice of the local coordinate system with the y axis pointing along Cu-O(3) and the x axis pointing along the Cu-Cl bond within the square plane.

$=105.7°$ for Cu-45124(Cl) and $\angle$Cu-O(1)-Cu$=109.8°$ for Cu-2252(Cl)]. The intratetrahedral hopping t_2 which was weak for Cu-2252(Cl)—a fact also supported by neutron diffraction[10]—remains weak for Cu-45124(Cl). The in-plane intertetrahedral hopping t_x, remains in magnitude similar to its analog in Cu-2252(Cl) while other in-plane intertetrahedral hoppings like t_a and t_r get suppressed. The out-of-plane, intertetrahedral hopping t_c remains more or less the same as in Cu-2252(Cl), while the t_z hopping increases by a factor of 2. The most remarkable change is observed for the diagonal hopping, t_d, which is reduced to 7 meV in Cu-45124(Cl) compared to a value of 80 meV in the Cu-2252(Cl) compound. This reduction, however, is not caused by the elongation of the bond lengths due to the insertion of the Te(1)O_4

TABLE I. Cu-Cu hopping parameters corresponding to the massively downfolded Cu-$d_{x^2-y^2}$ Hamiltonian. The bond lengths are in Å and the hopping interaction strengths are in meV corresponding to hoppings shown in Figs. 1 and 2. The values for Cu-2252(Cl) have been reproduced from Ref. 6.

	Cu-45124(Cl)		Cu-2252(Cl)	
	Bond length	Interaction	Bond length	Interaction
t_1	3.147	76	3.229	98
t_2	3.523	4	3.591	0
t_x	5.539	12	4.163	−10
t_a	6.180	15	6.021	−29
t_d	7.834	7	8.033	−80
t_r	8.251	18	9.048	−48
t_z	5.063	24	5.015	12
t_c	6.332	−48	6.320	−45

TABLE II. TB parameters in meV corresponding to two sets of calculations. Set 1: Massively downfolded Cu-$d_{x^2-y^2}$. Set 2: minimal set consisting of Cl-p and Cu-$d_{x^2-y^2}$ degrees of freedom (Cu+Cl downfolding). The numbers for Cu-2252(Cl) have been reproduced from Ref. 6.

	Cu-45124(Cl)		Cu-2252(Cl)	
	Cu	Cu+Cl	Cu	Cu+Cl
t_1	76	82	98	181
t_2	4	−117	0	−132
t_x	12	42	−10	−14
t_a	15	−39	−29	8
t_d	7	9	−80	8
t_r	18	−11	−48	−72
t_z	24	27	12	33
t_c	−48	−15	−45	−19

group in Cu-45124(Cl), as was suggested in Ref. 17. We reveal the origin of this marked difference in the following in terms of a detailed analysis of the involved hopping paths.

The tight-binding (TB) bands, constructed out of the hopping parameters tabulated in Table I are shown in the bottom panel of Fig. 5 in comparison to downfolded bands. The TB bands compare satisfactorily with the downfolded bands. Omission of long-ranged interactions such as t_c and t_r deteriorates the agreement of the TB bands with the downfolded bands, proving the essential need for inclusion of long-ranged interactions in the correct description of this compound.

INTERACTION PATHWAYS

It was pointed out in Ref. 6 that Cl-p degrees of freedom play a crucial role in the renormalization process of the effective Cu-Cu hopping. Keeping this fact in mind, we carried out downfolding calculations where the Cl-p degrees of freedom have been kept active in addition to Cu-$d_{x^2-y^2}$, so as to define a basis consisting of Cu-$d_{x^2-y^2}$ and Cl-p. The Cu-Cu hopping interactions extracted out of such calculation are tabulated in Table. II. For comparison, we show the results for Cu-2252(Cl) reproduced from Ref. 6. The crucial role of hopping paths involving Cl-p is evident by comparing the hopping interactions between the massively downfolded Cu-$d_{x^2-y^2}$-only calculation and the Cu-$d_{x^2-y^2}$+Cl-p calculation. The former includes the renormalization due to Cl-p's while the latter does not. While the pattern of renormalization remains essentially the same for the intratetrahedral hopping t_2 and the intertetrahedral out-of-plane hopping t_c, it is quite different for intertetrahedral hoppings like t_x, t_a, t_d, t_r, and t_z which involve pathways via Cl atoms belonging to two different Cu_4 tetrahedra. The most significant change happens for the in-plane intertetrahedral diagonal hopping, t_d. The bare hopping strength of t_d in absence of the renormalization effect of Cl-p is more or less the same between the two compounds [8 meV for Cu-2252(Cl) and 9 meV for Cu-45124(Cl)]. However, while a large renormalization is observed for Cu-2252(Cl) when integrating out the Cl-p degrees of freedom, such renormalization is practically absent in Cu-45124(Cl). This difference is caused—as pointed out previously—by the different alignment of the Cu-Cl bonds belonging to neighboring Cu_4 tetrahedra which are parallel to each other in Cu-45124(Cl) while in Cu-2252(Cl) they point to each other. *This makes the intertetrahedral Cl-p–Cl-p bonding in Cu-45124(Cl) of ppπ type as opposed to the Cu-2252(Cl) case, where the Cl-p–Cl-p bonding was of ppσ type*. This is nicely demonstrated in the Wannier function plot (see Fig. 7), where the effective Cu-$d_{x^2-y^2}$-like Wannier orbitals are placed at the Cu sites at in-plane diagonal positions. The relative orientation between the two orbitals provides a rough idea of the strength of the hopping matrix elements. In the case of Cu-2252(Cl), the Cl-p tails from two Cu sites belonging to two different Cu_4 tetrahedra point to each other due to direct alignment providing a Cl-p-Cl-p ppσ bonding which mediates the Cu-Cu bonding between different Cu_4 tetrahedra. For Cu-45124(Cl), in contrast, the Cl-p tails from different Cu sites belonging to two different Cu_4 tetrahedra have practically negligible contribution in the effective Cu-Cu bonding due to misalignment of the Cl-p tails.

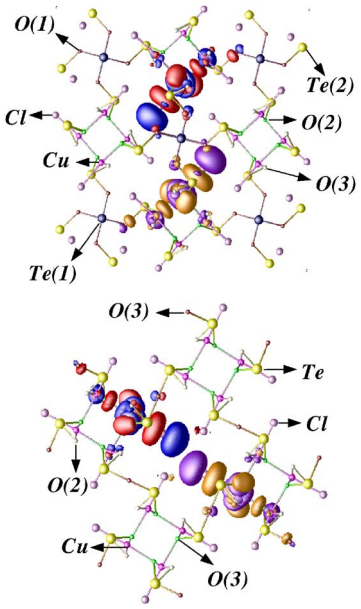

FIG. 7. (Color online) Overlap between Cu-$d_{x^2-y^2}$ downfolded *N*MTOs, placed at two Cu sites situated at in-plane intertetrahedral, diagonal positions. Opposite signed lobes of the orbitals are colored as blue (black) or magenta (dark gray) and red (gray) or orange (light gray).

The nature of the discussed interaction paths plays a crucial role in the magnetic properties of this material. Starting from the hopping parameters, t's, the exchange integrals, J's, for antiferromagnetic superexchange paths may be estimated by making use of the expression $J \approx 4t^2/U$. While this is a valid approach for cases like the t_1 and t_2 interaction paths, in general for more complicated paths this expression is not anymore precise and one has to use more involved estimations of the exchange coupling constants. Nevertheless, already the knowledge of the hopping parameters gives us the

clue about the important interaction paths. The drastic reduction of the in-plane t_d and to a lesser extent of t_a and the longer-ranged t_r, in Cu-45124(Cl) compared to Cu-2252(Cl), indicate an overall weakening of the intertetrahedral coupling in the Cu-45124(Cl) compound with respect to Cu-2252(Cl) and therefore if the system orders at low temperatures, the ordering should occur at a lower T_N than in Cu-2252(Cl), as observed experimentally.[17] The spin ordering patterns will be also strongly influenced by the change of interaction paths, especially by the near absence of the t_d and reduction of the t_a path (we refer to the discussion in Ref. 13) which places the system in the limit of weakly coupled tetrahedra. Also the reduction by 22% of the t_1 value implies a smaller intratetrahedron exchange coupling J_1 than in Cu-2252(Cl). By considering $J \approx 4t^2/U$, with $U=4$ eV we obtain as exchange coupling constants $J_1 \approx 5.8$ meV=67 K and $J_2 \approx 0.02$ meV=0.2 K in comparison with the values $J_1 = 2.84$ meV=32.9 K and $J_2 = 1.58$ meV=18.4 K obtained by fitting the susceptibility of a model of independent tetrahedra to the experimental data.[17] The ratio of J_2/J_1 is largely overestimated in the fitting, presumably because of the neglect of the intertetrahedral interactions.

Br SYSTEM

In an attempt to predict the properties of the not-yet-synthesized $Cu_4Te_5O_{12}Br_4$ [Cu-45124(Br)] and motivated by the discussed proximity to a quantum critical behavior of the recently studied $Cu_2Te_2O_5Br_2$ [Cu-2252(Br)], we have investigated the electronic and magnetic properties of the *ab initio* relaxed structure Cu-45124(Br) obtained from first principles calculations. In order to obtain a theoretical prediction of the Cu-45124(Br) crystal structure, we substituted Cl by Br in the original Cu-45124(Cl) structure and we relaxed the volume and internal coordinates by performing Car-Parrinello *ab initio* molecular dynamics (AIMD) calculations[20] with a projector augmented wave basis set.[21] This procedure has proven to be very suitable for predicting reliable crystal structures.[22] For Cu-45124(Br) we assumed the same tetragonal space group $P4/n$ (No. 85) as for Cu-45124(Cl). Of the seven atoms in the primitive cell, only Te(1) is in Wyckoff position $2c$, while all others [Te(2), Cu, Br, O(1), O(2), O(3)] are in position $8g$. We thus have 19 degrees of freedom, but as the AIMD relaxation is done in the conventional cell, we need 131 constraints for the 50 atoms in order to preserve the symmetry. We verified convergence of our structure relaxation not only with the help of the forces but we checked that each of the 19 independent coordinates has converged. This is especially important in this structure as we find that the relaxation happens in two steps. First, immediately after the Br atoms introduced into the Cl positions, they rearrange, increasing their bond distance to the Cu atoms which are the nearest neighbors. This Cu-Br repulsion makes an adjustment of the O(1) positions next to Br and the O(2) and O(3) positions next to Cu necessary. However, in course of further AIMD iterations, while the Br atom moves further and finds a relatively favorable position, some changes to Cu and O(1)-O(3) coordinates are actually reversed. Thus, the structure immediately following the first fast rearrangement would have produced quite different interactions strengths than the final relaxed structure given in Table III. As would be expected from the different radii of Br and Cl atoms, we find the largest adjustments in the Br atom positions which change by 0.16 Å during the relaxation. The other changes are 0.05 Å for Te(1), 0.04 Å for Te(2), 0.04 Å for Cu, 0.10 Å for O(1), 0.04 Å for O(2), and 0.07 Å for O(3). While the volume of the Cu-45124(Br) structure shows a negligible change with respect to the volume of Cu-45124(Cl), appreciable changes in bond lengths and angles are observed. The Cu-O(2) distance which alternates between 1.94 and 2.01 Å in Cu-45124(Cl), becomes 1.91 and 2.01 Å in Cu-45124(Br). The Cu-O(3) distance is slightly smaller at 1.90 Å [from 1.91 Å in Cu-45124(Cl)]. The Cu-O(2)-Cu angle changes from 105.7° in Cu-45124(Cl) to 107.2° in Cu-45124(Br), while the O-Cu-O angle stays nearly constant at 87.0°/[87.1° in Cu-45124(Cl)]. While the Cu-Cl distance is 2.24 Å, the Cu-Br distance is 2.42 Å. Finally, the Cl-O(1) distances alternate between 3.27 and 3.40 Å while the Br-O(1) distances are 3.22 and 3.55 Å. In Table III we present the relaxed coordinates of Cu-45124(Br).

TABLE III. Fractional coordinates obtained by AIMD of the relaxed Cu-45124(Br).

	x	y	z
Te(1)	0.25	0.25	0.376 603 83
Te(2)	0.673 708 04	0.018 727 271	0.870 864 73
Cu	0.755 879 33	0.405 102 64	0.348 174 24
Br	0.893 550 65	0.566 809 22	0.323 075 12
O(1)	0.295 317 85	0.406 097 92	0.232 738 45
O(2)	0.283 841 54	0.872 386 49	0.361 011 69
O(3)	0.291 597	0.580 808 43	0.938 937 75

We performed NMTO-downfolding for this system and in Tables IV and V we present the bond distance and hopping values together with those of [Cu-2252(Br)]. Both a Cu-

TABLE IV. Cu-Cu hopping parameters corresponding to the massively downfolded Cu-$d_{x^2-y^2}$ Hamiltonian. The bond lengths are in Å and the hopping interaction strengths in meV corresponding to hoppings shown in Figs. 1 and 2. The numbers for Cu-2252(Br) have been reproduced from Ref. 6.

	Cu-45124(Br)		Cu-2252(Br)	
	Bond length	Interaction	Bond length	Interaction
t_1	3.147	75	3.195	80
t_2	3.522	0	3.543	4
t_x	5.535	23	4.385	−16
t_a	6.248	20	6.289	−30
t_d	7.829	3	8.439	−73
t_r	8.251	−29	9.130	−35
t_z	5.064	19	5.059	11
t_c	6.332	−39	6.378	−48

TABLE V. Cu-Cu hopping parameters in meV corresponding to two sets of calculations. Set 1: Massively downfolded Cu-$d_{x^2-y^2}$. Set 2: Minimal set consisting of Br-p and Cu-$d_{x^2-y^2}$ degrees of freedom (Cu+Br downfolding). The numbers for Cu-2252(Br) have been reproduced from Ref. 6.

	Cu-45124(Br)		Cu-2252(Br)	
	Cu	Cu+Br	Cu	Cu+Br
t_1	75	106	80	155
t_2	0	−60	4	−156
t_x	23	−15	−16	−10
t_a	20	−16	−30	5
t_d	3	11	−73	8
t_r	−29	−16	−35	−62
t_z	19	68	11	34
t_c	−39	−53	−48	−26

$d_{x^2-y^2}$ and a Cu-$d_{x^2-y^2}$+Br-p downfolding were performed.

Cu-45124(Br) shows the same trend as Cu-45124(Cl) regarding the intertetrahedral hopping t_d, namely the near absence of Cu-Cu interaction along this path. The rest of the in-plane intertetrahedral hopping paths in Cu-45124(Br) are a bit larger than in Cu-45124(Cl) but, except for t_x, they are smaller than in Cu-2252(Br). From the knowledge of the previous systems, a phase transition to an ordered state is also to be expected for this system at low temperatures.

An important issue to be mentioned at this point is the value of the intratetrahedron ratio t_2/t_1 in all the compounds discussed here. Large values of this ratio can be related to an enhancement of intratetrahedron frustration, what has been already discussed for Cu-2252(Br).[6] Cu-2252(Br) is found to have a small but nonzero t_2 in comparison to its value for Cu-2252(Cl), where the t_2 hopping path is basically zero, mainly due to the Cl renormalization. The present set of systems, i.e., the synthesized Cu-45124(Cl) and the *ab initio* computer designed Cu-45124(Br) seem to behave in the opposite way. While Cu-45124(Cl) has a small but nonzero t_2, Cu-45124(Br) relaxes into a structure where the t_2 path is completely renormalized to zero by the hybridization with the Br ions (see Table V) in the square planar configuration. Though we found an interesting transient structure for Cu-45124(Br) with a moderate intratetrahedron t_2/t_1, this does not seem to be the energetically favored structure within the AIMD approach.

Finally, we note that the value of the *ab initio* calculated hopping parameters is very susceptible to small changes of distances and angles between the atoms. Our AIMD calculations were performed within the GGA approximation. Consideration of other exchange correlation potentials may change slightly the relaxed structure, which could be important especially for the intratetrahedron hopping paths, where changes of 0.02 to 0.03 Å in the distance between Cu and O(2) and of 2.9° in the Cu-O(2)-Cu angle are decisive for the variation of the hopping parameters.

SUMMARY

To conclude, we have made a comparative study between the spin tetrahedron system $Cu_2Te_2O_5Cl_2$ and a recently synthesized compound $Cu_4Te_5O_{12}Cl_4$ in terms of the microscopic analysis of the electronic structure. Our study shows that although the basic nature of the interactions remains the same, there is a drastic reduction of the in-plane intertetrahedral diagonal interaction in comparison to the case of $Cu_2Te_2O_5Cl_2$ where this diagonal interaction was estimated to be nearly as strong as the Cu_4 intratetrahedral nearest-neighbor interaction t_1. We show that the origin of this reduction is due to subtle changes in the crystal structure of $Cu_4Te_5O_{12}Cl_4$ which cause Cu-Cl bonds belonging to different Cu_4 tetrahedra to align in parallel in the $Cu_4Te_5O_{12}Cl_4$ compound rather than pointing toward each other as was the case in $Cu_2Te_2O_5Cl_2$. This reduction of the in-plane diagonal hopping in turn increases the importance of the out-of-plane hopping to the extent that some intertetrahedral hoppings along [001] (t_c) are even about three times stronger than those within the plane.

In absence of the yet-to-be-synthesized $Cu_4Te_5O_{12}Br_4$, and motivated by the more anomalous properties observed in the Br analog to $Cu_2Te_2O_5Cl_2$, we have theoretically derived the hypothetical crystal structure of $Cu_4Te_5O_{12}Br_4$ by performing a geometry relaxation in the framework of *ab initio* molecular dynamics. We have analyzed the electronic properties of this system within the NMTO downfolding procedure. We observe that, while the overall electronic and magnetic behavior seems to be similar to its Cl sister compound, this computer designed Br system shows (except for t_d) a stronger in-plane intertetrahedron interaction than the Cl system—an effect that was also observed in the comparison between $Cu_2Te_2O_5Br_2$ and $Cu_2Te_2O_5Cl_2$. However we do not observe any noticeable effect on the intratetrahedron frustration in the final relaxed $Cu_4Te_5O_{12}Br_4$ structure.

ACKNOWLEDGMENTS

We would like to thank P. Lemmens and M. Johnsson for very fruitful discussions. R.V. thanks the German Science Foundation (DFG) for financial support. B.R. and T.S.D thanks the MPG-India partner-group program for the collaboration. T.S.D thanks the Swarnajayanti group for financial support. H.O.J. gratefully acknowledges support from the DFG through the Emmy Noether program. We gratefully acknowledge support by the Frankfurt Center for Scientific Computing.

[1] See for a recent review, R. Moessner and A. Ramirez, Phys. Today **59** (2), 24 (2006).
[2] M. Johnsson, K. W. Törnroos, F. Mila, and P. Millet, Chem. Mater. **12**, 2853 (2000).
[3] P. Lemmens, K.-Y. Choi, E. E. Kaul, C. Geibel, K. Becker, W. Brenig, R. Valentí, C. Gros, M. Johnsson, P. Millet, and F. Mila, Phys. Rev. Lett. **87**, 227201 (2001).
[4] W. Brenig and K. W. Becker, Phys. Rev. B **64**, 214413 (2001).
[5] C. Gros, P. Lemmens, M. Vojta, R. Valentí, K. Y. Choi, H. Kageyama, Z. Hiroi, N. Mushnikov, T. Goto, M. Johnsson, and P. Millet, Phys. Rev. B **67**, 174405 (2003).
[6] R. Valentí, T. Saha-Dasgupta, C. Gros, and H. Rosner, Phys. Rev. B **67**, 245110 (2003).
[7] See, for instance, T. Saha-Dasgupta, R. Valentí, F. Capraro, and C. Gros, Phys. Rev. Lett. **95**, 107201 (2005).
[8] J. Jensen, P. Lemmens, and C. Gros, Europhys. Lett. **64**, 689 (2003).
[9] V. N. Kotov, M. E. Zhitomirsky, M. Elhajal, and F. Mila, Phys. Rev. B **70**, 214401 (2004).
[10] O. Zaharko, A. Daoud-Aladine, S. Streule, J. Mesot, P.-J. Brown, and H. Berger, Phys. Rev. Lett. **93**, 217206 (2004).
[11] S. J. Crowe, M. R. Lees, D. M. K. Paul, R. I. Bewely, J. Taylor, G. McIntyre, O. Zaharko, and H. Berger, Phys. Rev. B **73**, 144410 (2006).
[12] O. K. Andersen and T. Saha-Dasgupta, Phys. Rev. B **62**, R16219 (2000); O. K. Andersen, T. Saha-Dasgupta, and S. Ezhov, Bull. Mater. Sci. **26**, 19 (2003).
[13] O. Zaharko, H. Ronnow, J. Mesot, S. J. Crowe, D. McK. Paul, P. J. Brown, A. Daoud-Aladine, A. Meents, A. Wagner, M. Prester, and H. Berger, Phys. Rev. B **73**, 064422 (2006).
[14] P. Lemmens, K.-Y. Choi, G. Güntherodt, M. Johnsson, P. Millet, F. Mila, R. Valentí, C. Gros, and W. Brenig, Physica B **329**, 1049 (2003).
[15] J. Kreitlow, S. Süllow, D. Menzel, J. Schoenes, P. Lemmens, and M. Johnsson, J. Magn. Magn. Mater. **290**, 959 (2005).
[16] X. Wang, I. Loa, K. Syassen, P. Lemmens, M. Hanfland, and M. Johnsson, J. Phys.: Condens. Matter **17**, 807 (2005).
[17] R. Takagi, M. Johnsson, V. Gnezdilov, R. K. Kremer, W. Brenig, and P. Lemmens, Phys. Rev. B **74**, 014413 (2006).
[18] Please note that we used the atom labeling given in Refs. 2 and 17.
[19] Stuttgart LMTO code, O. K. Andersen and O. Jepsen, Phys. Rev. Lett. **53**, 2571 (1984).
[20] R. Car and M. Parrinello, Phys. Rev. Lett. **55**, 2471 (1985).
[21] P. E. Blöchl, Phys. Rev. B **50**, 17953 (1994).
[22] L. A. Salguero, H. O. Jeschke, R. Valentí, B. Rahaman, T. Saha-Dasgupta, C. Buchsbaum, and M. U. Schmidt, cond-mat/0602633.